

CATALOGUING PERFORMANCE ASSESSMENT METHOD OF SST SENSOR NETWORKS

Daniel Sáez-Bo ^a, Diego Escobar ^a, Alejandro Pastor-Rodríguez ^a, Francisco Ayuga-García ^a

^a GMV, Calle Isaac Newton 11, Tres Cantos, 28670, Spain

ABSTRACT

The **performance** of SST architectures is typically measured in terms of number of **observable objects** and number of **catalogable objects**. By definition, an object is considered observable if the sensor network can observe the object at least once and generate the corresponding track. Similarly, an object is considered catalogable if it can be maintained in the catalogue through the update of its orbital information upon the generation of tracks corresponding to the object during survey observation activities.

Many previous studies state that an object is catalogable if its **revisit time** is lower than **24 hours**. However, this assumption is not properly justified. Apart from the catalogability of an object, another aspect to consider is the accuracy of the orbital information being estimated from the correlated observations.

This paper presents a new methodology suited for Low Earth Orbit (LEO) and developed to determine through a coverage analysis the population of objects that can be catalogued by a given sensor network, as well as the expectable accuracy of the orbital information generated from observations of the sensor network.

Index Terms — space debris, space surveillance and tracking, cataloguing capabilities, catalogue maintenance, sensor network performance

1. INTRODUCTION

The European Union is now developing a federated **Space Surveillance and Tracking (SST) system** composed of existing sensors and operations centres in Europe through the EU SST Support Framework. Potential future architectures are also being evaluated for the development of new future sensors, including both **radar and telescope sensors** and both tracking and surveillance sensors. This brings the need to analyse the performances of different sensor network architectures and topologies.

One of the most important features of a Space Surveillance and Tracking (SST) system is the capability to catalogue objects. The cataloguing capability strongly depends on the **revisit time** (time between two consecutive observations of an object) for a given object population. Furthermore, it is also driven by the ability of the on-ground infrastructure maintaining the catalogue to predict the orbits of the objects, depending on the accuracy of the sensors' measurements and of the predictions of solar flux and magnetic field activity.

2. OBJECTIVE

The objective of this work is the development of a **systematic method** to estimate the **performance and cataloguing capabilities of SST systems** and in particular, radar systems devoted to SST tasks. Current analyses of cataloguing capabilities tend to be oversimplified and the criteria to decide whether an object can be catalogued or not is not accurate enough to give a good estimation of the real performance of the system. A fixed maximum allowable revisit time of 1 day is usually set as reference [1].

This work presents a different criteria which aims to improve the results of these performance estimations by taking into account the **uncertainty** in the object's position, through the **orbital semi-major axis uncertainty** and the **number of objects** in the vicinity of the object to estimate a different maximum allowable revisit time for each orbital altitude. Under this criteria, an object can be maintained in the catalogued only if its **expected revisit time** is below the **maximum allowable revisit time** for its orbital altitude.

Additionally, this new criteria is applied to the study of the main design parameters of an SST radar: radar location (i.e. latitude), field of view (i.e. pointing elevation), power and the predicted orbit uncertainty (i.e. accuracy of measurements). Their effect on the allowable revisit time and on the SST cataloguing capabilities give some guidelines on which are the best choice for these parameters.

2.1. Sensor location and Field of view pointing

First, the radar **location, Field of View (FoV) and power** constrain the orbit observability and revisit times. Depending on the location and FoV of the radar, the **expected revisit times** of the observable population vary. This drastically affects the capability of the SST system to maintain the objects in the catalogue by correlating the observations to the right object of the catalogue. The longer the revisit time, the more difficult it is to correlate the observations correctly. Hence, it is necessary to decide the radar location and field of view (size and elevation) considering this constraint.

A **parametrical analysis** on the latitude and the elevation of the field of view with three radars with different power has been performed as part of this study.

2.2. Orbit semi-major axis uncertainty

Second, the orbit uncertainty, characterised mainly by the **semi-major axis uncertainty**, determines the **maximum allowable revisit time** for the proper correlation between observations and catalogued objects. The two main uncertainty contributors in LEO are the initial error in the semi-major axis, characteristic of the sensor network, and the atmospheric drag uncertainty.

On the one hand, the **initial semi-major axis error** is related to the observability of the orbit of the objects from the sensor network considered as well as with the accuracy of the sensors considered. The accuracy of radar measurements cannot be mapped directly to the accuracy of the semi-major axis, although it is related to it through common orbit determination techniques.

On the other hand, the **drag-induced uncertainty**, of special importance for Low Earth Orbit (LEO) objects, relies on atmosphere models and its uncertainty, which require **Space Weather conditions** information. The most usual parameters considered for this are the **solar flux** at a wavelength of 10.7 cm and the **magnetic field activity** Ap index. The accuracy in their predictions needs to be bounded to obtain a reliable estimation of the effect of the drag uncertainty on the orbit's uncertainty evolution.

To estimate the uncertainty in these predictions, an analysis of the solar flux and Earth magnetic field predictions and their impact on the semi-major axis uncertainty was performed and their relationship with the atmospheric models assessed. This study has been useful to justify some of the parameters fixed for the SST system performance analysis, in particular, the expected uncertainty in the semi-major axis due to drag effects.

3. PHYSICAL MODEL

The proposed model for the estimation of the performance of a network of SST sensors is based on the estimation of the **maximum allowable revisit time** (maximum time interval acceptable between orbital information updates for a given object) compared with the **expected revisit time** (expected time between re-observations of an object). The rationale behind this is that as the position uncertainty of two objects do not overlap, the measurements will be successfully correlated during the correlation process, allowing to maintain the object in the catalogue.

Therefore, this analysis is independent of the specific correlation method and provides a fast preliminary evaluation. A more realistic cataloguing performance analysis would make use of the correlation algorithms used for the tracks and objects association.

3.1. Model assumptions

The following assumptions have been considered for this analysis, focused in LEO orbital regime:

- Orbits are considered **circular** based on the fact that the object population considered has in all cases an eccentricity below 0.1, with a much higher density of values below 0.02 (>80%).
- The maximum allowable revisit time to achieve successful correlation is computed assuming that all objects are **uniformly distributed** along slots defined by their orbit altitude and Right Ascension of the Ascending Node (RAAN), and considering the time it takes for the position uncertainty along the orbit to overlap between consecutive objects.
- The **main orbital perturbation** driving the increase in uncertainty in the position of the object is the **initial semi-major axis uncertainty and the atmospheric drag**, both due to uncertainties in the estimation of the drag effect on the objects and in the prediction of the solar flux and magnetic activity which controls the atmospheric density.
- Steps of 100 km in altitude and 36 degrees in RAAN to define the considered orbits have been used for the semi-major axis.
- The **area to mass ratio** used for the analysis has been derived from the actual objects population, using the value obtained to cover 66% of the observable population, resulting in a value of 0.08 m²/kg. This value is higher than the typical reference value (0.015 m²/kg), but ensures covering a larger part of the observable population.
- A typical value of 2.2 is used for the **drag coefficient**, and a 50% of uncertainty in the estimation of the drag coefficient and prediction of the atmospheric density is used as reference, as derived from the Space Weather uncertainty prediction analysis presented in section 4.

3.2. Radar field of view modelling

The **radar FoV** is modelled as a **pyramid** in the radar antenna reference frame. The radar reference distance and reference radar cross section parameters allow to determine the minimum signal required to be received from an object echo to be detected. Applying the radar equation [2], the **detection condition** can be expressed as:

$$\frac{RCS}{r^4} \geq \frac{RCS_{ref}}{r_{ref}^4} \propto SNR_{min} \quad (1)$$

where RCS is the object radar cross section, r is the distance between the object and the sensor and SNR_{min} is the minimum radar Signal to Noise Ratio required for the object detection. For an object to be detected, it must lie within the sensor FoV.

3.3. Maximum allowable revisit time determination

The following paragraphs describe the formulation used to derive the **maximum allowable revisit time** for an object to be considered as catalogued with the assumptions above.

An uncertainty in the semi-major axis, σ_a , leads to an increase over time in the uncertainty in the position along the orbit, σ_{along} , as:

$$\frac{d\sigma_{along}}{dt} = \frac{n_0}{2} \sigma_a \quad (2)$$

where n_0 is the mean motion of the unperturbed orbit.

This expression can be easily derived from the expression of the along-track velocity of an object in a circular orbit:

$$v_{along} = \frac{ds}{dt} = n_0 a_0 = \sqrt{\frac{\mu}{a_0}} \quad (3)$$

where a_0 is the semi-major axis of the unperturbed orbit, μ is Earth's gravitational parameter and s is the arc coordinate along the orbit.

The uncertainty of the semi-major axis depends on the initial uncertainty, $\sigma_{a,0}$ and the uncertainty in the effect of the atmospheric drag on the object, $\sigma_{a,drag}$. The former is constant along time while the latter increases over time according to:

$$\sigma_{a,drag}(t) = \sqrt{\mu a_0} \frac{A}{m} C_{d0} \rho_0 \sigma_{Cd\rho,r} t = \frac{d\sigma_{a,drag}}{dt} t \quad (4)$$

where C_{d0} is the reference drag coefficient (i.e., 2.2 as assumed above), ρ_0 is the reference atmospheric density for that altitude, $\frac{A}{m}$ is the area-to-mass ratio, t is the time since the last orbit determination, $\sigma_{Cd\rho,r}$ is the uncertainty in the estimated drag coefficient and the prediction of the atmospheric density, expressed as a percentage with respect to the reference values (i.e., 50% as assumed above).

This last expression can be easily derived from orbital energy considerations, taking into account the rate of change in energy of a circular orbit caused by atmospheric drag. Both uncertainties can be combined as usual as:

$$\sigma_a = \sqrt{\sigma_{a,0}^2 + \sigma_{a,drag}^2} \quad (5)$$

Substituting σ_a by this expression in time the derivative of the along-track direction uncertainty, σ_{along} , and integrating the resulting expression one gets:

$$\sigma_{along}(t) = \sigma \left(\sigma_{a,0}, \frac{d\sigma_{a,drag}}{dt}, t \right) + \sigma_{along,const} \quad (6)$$

where $\sigma \left(\sigma_{a,0}, \frac{d\sigma_{a,drag}}{dt}, t \right)$ is a function composed by a lineal term and a logarithmic term that depends on the initial uncertainty in the semi-major axis, the time derivative of the uncertainty contribution due to drag effects and time.

Defining:

$$K1 = \sigma_{a,0}^2$$

$$K2 = \left(\sqrt{\mu a_0} \frac{A}{m} C_{d0} \rho_0 \sigma_{Cd\rho,r} \right)^2 \quad (7)$$

Then $\sigma \left(\sigma_{a,0}, \frac{d\sigma_{a,drag}}{dt}, t \right)$ can be written as:

$$\sigma \left(\sigma_{a,0}, \frac{d\sigma_{a,drag}}{dt}, t \right) = \frac{n_0}{2 \cdot 2} \left(t \cdot \sqrt{K1 + K2 \cdot t^2} \right) + \frac{K1 \cdot \log(\sqrt{K2} \sqrt{K1 + K2 \cdot t^2} + K2 \cdot t)}{\sqrt{K2}} \quad (8)$$

Finally, the maximum allowable revisit time is obtained when the 3-sigma along-track uncertainty equals the separation between two consecutive objects in the orbit, that is:

$$\frac{\pi a_0}{N_{obj}} = 3 \left(\sigma \left(\sigma_{a,0}, \frac{d\sigma_{a,drag}}{dt}, t_{max} \right) + \sigma_{along,const} \right) \quad (9)$$

with N_{obj} being the number of objects in the altitude slot under consideration. This last implicit expression allows to obtain the **maximum allowable revisit time** for correlation purposes at a given altitude window.

4. RESULTS

First, the results of the **Space Weather indicators predictions uncertainty** analysis is presented to determine the typical uncertainty in the drag estimation. For this analysis historical data since 1996 for the solar flux F10.7 and the Ap magnetic activity indicator from NOAA [3] was used as reference (covering a complete Solar Cycle) and prediction intervals from 1 to 30 days were studied.

For the **cataloguing performance analysis**, a population containing 12,770 objects from the JFSCC TLE [4] catalogue was used. This represents around a 76% of the total number of objects, which corresponds with almost all the LEO objects in the JFSCC catalogue.

Three different radar systems have been defined for this analysis. The only difference between them is the power (i.e. their range and size detection thresholds). Table 1 summarizes the characteristics of each of them. The accuracy of the measurements is assumed to be of the order of 10 m for the three systems.

Table 1: Radar systems characteristics

Radar	Ref. Diameter	Ref. RCS	Ref. Distance
Radar 1	L m	A m ²	1000 km
Radar 2	L/4 m	A/16 m ²	1000 km
Radar 3	L/16 m	A/256 m ²	1000 km

The more powerful the radar is, the more objects it will be able to detect and more passes will be generated. However, the **correlation success** may decrease as **more objects are observed**, since it is more difficult to unequivocally determine to which object the measurements correspond during the correlation process. Additionally, the **allowable revisit time** to maintain the error in the required range decreases with the increase of the **number of observed objects**, due to the higher object density.

For the three radars, a total of 304 different cases for each one was simulated with a combination of radar latitudes ranging from 0° N to 90° N and radar FoV pointing elevations from 10° to 85°, in steps of 5° in both cases.

The following paragraphs highlight the most relevant findings that can be extracted from **this preliminary performance analysis** for a SST radar.

4.1. Space weather predictions uncertainty

Solar Flux F10.7 prediction uncertainty

The **relative difference of the F10.7 predictions** with respect to the observed value for each day is shown in Figure. The histogram for the whole interval data for each prediction range from 1 to 30 days was obtained and a normal distribution was adjusted, grouping the data with a sliding sampling window of 30 days and the 68% confidence interval (equivalent to 1-sigma confidence level) was taken as reference.

The colour scale represents the **relative difference** for the 68% interval, ranging from 0%, in blue, to the 20% in red. The x-axis represents the day of the event and the y-axis gives the prediction time from one to thirty days. The second plot, shows the solar activity for the same time interval.

As it can be observed, during the **solar maxima period**, from 1999 to 2006 and 2011 to 2017, the noise in the F10.7 observed data is greater than the **solar minima periods**. This has also an impact on the error of the predictions, as it is clearly seen in the first plot. For forecasts for 5 and more days ahead, the relative error can vary from the $\pm 20\%$ and more during the solar maxima to only $\pm 5\%$ during the solar minima, for the 68% confidence interval. However, the **one day prediction** remains bounded around the **$\pm 5\%$ relative difference** all the time.

The relative difference for **one day prediction** has been taken as reference since, for cataloguing purposes, the usual maximum prediction time required is the interval between F10.7 measurements update, which is usually one day.

Ap index prediction uncertainty

Figure shows a similar analysis performed for the **Ap index prediction uncertainty**. The time-evolution of the error showed that the uncertainty in the prediction is, in general,

not improved as the time of the event gets closer and it remains almost constant independently of the prediction time. In some cases, the error in the estimation is above the 200%. In most of the cases, for the 5-day prediction an improvement is observed to values of around 70%-100% error in most of the cases for the 68% interval.

For the one day prediction, which is the most relevant for the cataloguing capabilities analysis, a **reference value of 50%** is taken for the Ap estimations.

Space Weather indicators impact on the drag estimation

Additionally to the **uncertainty of the atmospheric models** themselves, which in the literature is usually estimated around 15%-30% for most of the models [5,6], the impact of the **propagation of the uncertainties in the Space Weather indicators** has to be determined and their effect on the density estimation. To do so, a reference orbit has been defined at different altitudes, ranging from 200 to 2000 km, and propagated with increments in the F10.7 flux and the Ap index with respect to a reference value to compute how the density estimation for the propagation and drag computation are affected by this variation.

Once the acceleration due to the aerodynamic forces time evolution has been simulated, the **root mean square difference** with respect to the reference orbit is computed for each altitude and this value is taken as reference of the impact of the variation of this parameter.

Figure 1 shows the result of the **sensitivity analysis**. In blue the root mean square of the time evolution for each altitude corresponding to the 1-sigma errors in the estimation for both indexes (5% for the f10.7 flux and 50% for the Ap index). The red line shows the corresponding root mean square difference across altitudes.

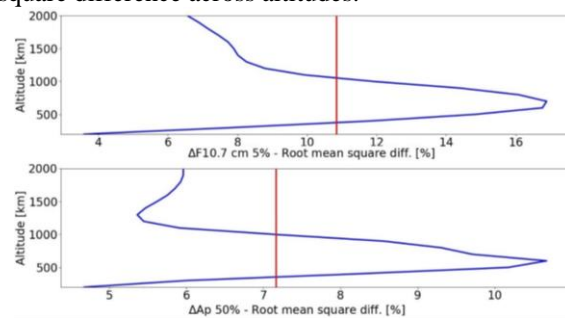


Figure 1: Root mean square difference for 5% increment in F10.7 (top) and 50% Ap (bottom)

Variations in the F10.7 cm flux estimation have greater impact in the orbit propagation and estimated aerodynamic acceleration than changes in the Ap index. A **5% difference in the F10.7 flux** can cause an **increment in the acceleration due to drag of 17%**, while an error in the **Ap of 50%** causes a **variation in the acceleration up to 11%** with respect the reference value.

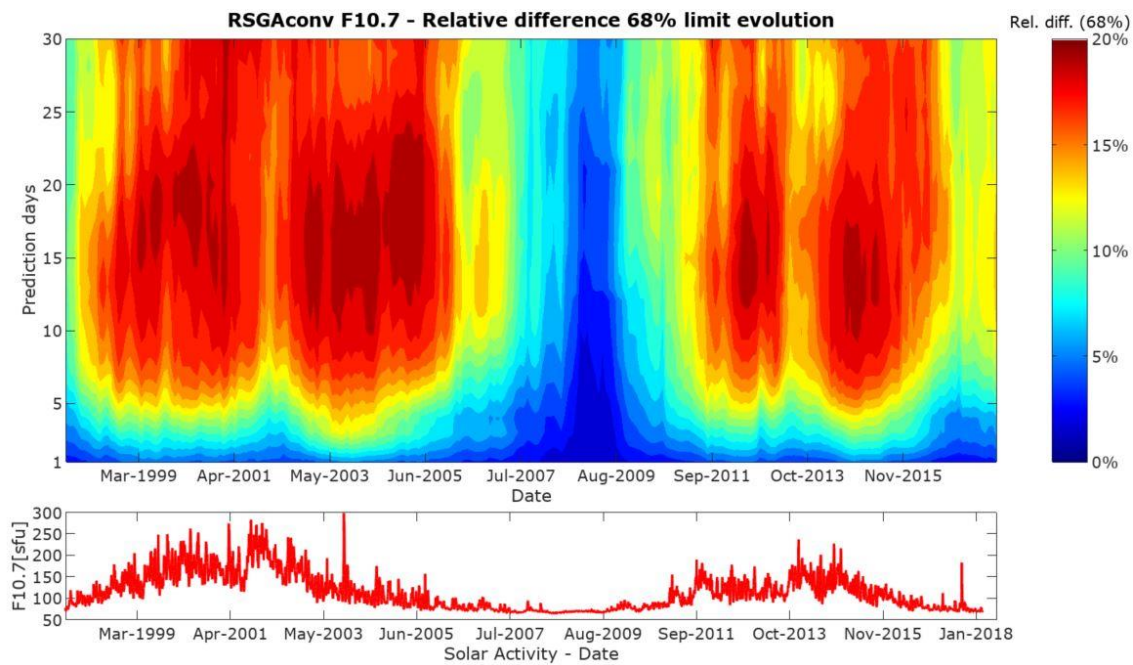


Figure 2: F10.7 Relative difference for the time evolution of the 68% interval throughout the Solar Cycle

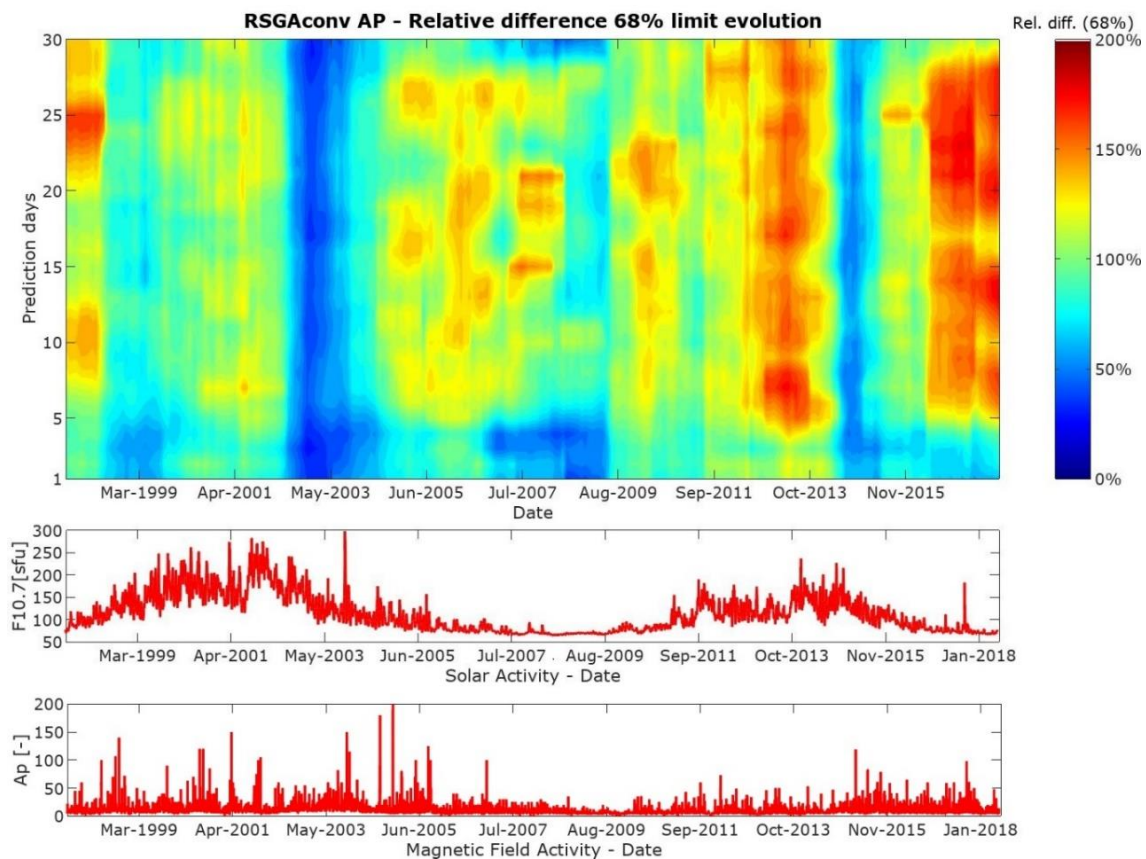


Figure 3: Ap Relative difference for the time evolution of the 68% interval throughout the Solar Cycle

Additionally to these two errors in the acceleration caused by the uncertainty in the values of the Space Weather indicators predictions, the uncertainty of the atmospheric models has to be added. Finally, the drag coefficient, area and object's mass has also an uncertainty associated to its estimation that must be taken into account for the propagation and drag effects. The total uncertainty in these magnitudes is estimated to be around a 10%. Computing the total uncertainty from these four values, around 40% uncertainty in the drag estimation can be expected from these sources.

A value of 50% in the drag uncertainty is chosen as figure of merit to take into account additional uncertainties and simplifications of the model.

4.2. Radar latitude and FoV pointing analysis

The main indicators of the system performance are the number of observed objects, the number of tracks generated, the tracks duration, the revisit times and the number of catalogued objects. The results presented hereafter correspond with an initial uncertainty in the orbit semi-major of 100 m and a 50% uncertainty in the drag estimation.

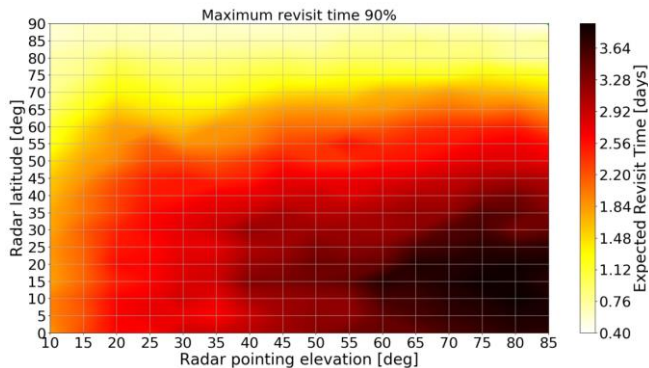


Figure 4: Maximum expected revisit time for 90% of objects in latitude and FoV elevation for Radar 2

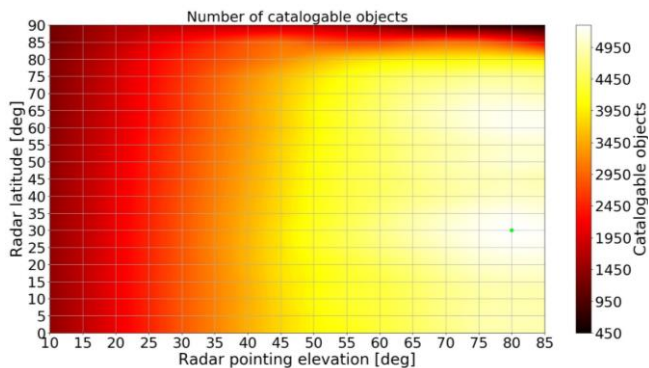


Figure 5: Number of catalogued objects in latitude and FoV elevation for Radar 2

As Figure suggests, in general, **lower latitudes** for the radar location are preferred in terms of number of observed objects as objects with lower inclinations can be observed, but as drawback, the **revisit time** tends to increase in this region. On the contrary, near-pole latitudes increase the number of tracks generated by the system and the radar utilization is improved as most of the objects can be observed in every orbital period because they follow nearly polar orbits, decreasing the objects' revisit times.

Increasing the **radar power** can improve the SST system cataloguing capabilities as smaller objects and objects at higher altitudes can be observed and catalogued, increasing the overall number of observed and catalogued objects.

However, this increase in the power must come with an **improvement in the orbit accuracy** (and hence measurements accuracy) as eventually, the uncertainty in the position of the objects will require too short revisit times, which will not be reachable with the sensor. **Increasing the accuracy in the semi-major axis determination** allows having **longer revisit times**. In other words, for a given sensor location and measurements accuracy, the **number of catalogable objects saturates** at a given point and does not increase even if the power is increased and more objects are observed, as shown in Figure. In order to increase further the number of catalogable objects, it is necessary to improve the measurements accuracy.

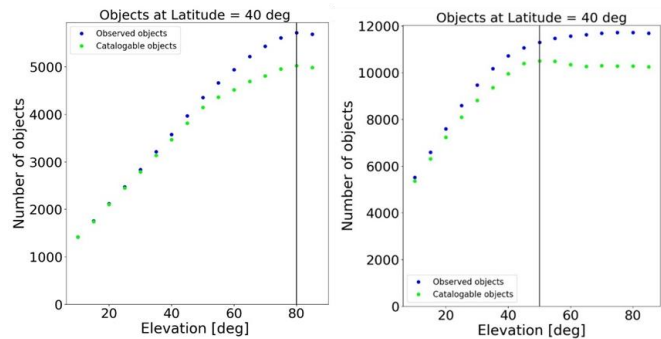


Figure 6: Comparison of observed and catalogued objects between radars 2 (left) and 3 (right) (saturation vertical line in bold) as a function of the FoV elevation and 40° latitude

There is a **trade-off** between the **number of detected** objects and the **maximum allowable revisit time**. It is desirable to have the maximum number of objects possible with the longer allowable revisit time possible to maintain the catalogue. However, increasing the number of objects detected, decreases the maximum allowable revisit time, while the expected revisit times remain unaffected, as they depend mainly on the orbit's characteristics and sensor location.

From the point of view of the **track duration**, having a **lower pointing angle of the FoV is preferable**, as this gives longer passes and thus measurements allow better correlation to maintain and update the orbits in the catalogue. However, as the FoV pointing angle is decreased (i.e. elevation of the field of view or tilt angle) the number of objects observed also decreases as the range increases, **losing the capability to observe smaller objects at a given altitude**.

Figure presents the number of observed and catalogued objects for one of the cases for radar 2. The number above each column gives the percentage of catalogued objects of the total observed objects at that altitude. The second number (in vertical) gives the maximum allowable revisit time for that specific altitude window, computed applying the proposed methodology.

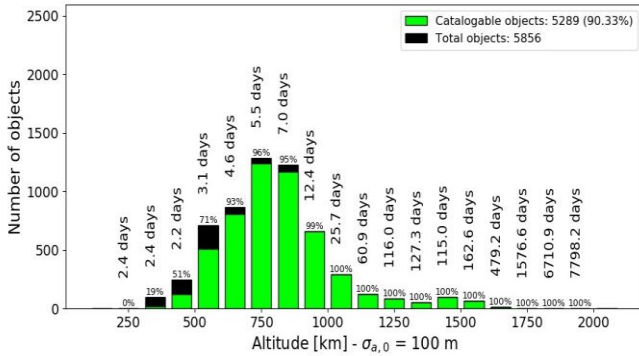


Figure 7: Number of catalogued objects with $\sigma_{\text{drag}} = 50\%$ and $\sigma_{a,0} = 100$ m

Table 2 presents the comparative results between the proposed criteria and the 1-day criteria. It can be observed that, in general, the 1-day criteria tends to estimate the system performance to be worse. The analysis also showed that the 1-day revisit time criteria tends to be too restrictive in low-populated regions and high-altitudes, where the expected revisit time tends to be longer and too permissive in high-populated regions.

Table 2: Maximum number of catalogued objects considering proposed and typical 1-day criterion

Radar	Maximum number of catalogued objects	
	Proposed criteria	1-day criteria
Radar 1	1 518 (11.89%)	1 018 (7.98%)
Radar 2	5 289 (41.42%)	3 996 (31.29%)
Radar 3	11 272 (88.27%)	10 281 (80.51%)

It has also been observed that the radar **optimum location might vary depending on the radar characteristics** and the orbital characteristics of the objects. For the three radars analysed with different power, the **optimal location** and FoV pointing elevation was: 30° latitude and 80° elevation for the least powerful radar as well as for the radar with intermediate

power (Figure), and 65° latitude and 75° elevation for the most powerful radar. The difference between both situations is due to the fact that radar 3 is saturated. This study was performed with the current debris distribution in LEO, a different future distribution might have relevant impact in the SST system performance and optimum design. Up to the 90% of the current LEO population of objects can be covered with a single SST radar with the proper configuration regarding power, location and FoV pointing elevations.

4.3. Orbit semi-major axis uncertainty impact analysis

Concerning the **uncertainties in the semi-major axis** (the initial and the drag-induced uncertainties), reducing both of them will improve the system cataloguing capabilities in general. However, depending on the number of objects in a given altitude region this may have not an effect at all, as the expected revisit time might remain higher than the maximum allowable revisit time. Furthermore, if all observed objects can be catalogued, further reducing the uncertainty is useless from the point of view of the cataloguing performance, as Figure 8 suggests.

In general, at lower altitudes, the uncertainty driving the **maximum allowable revisit time is the drag uncertainty** since the drag effect is more relevant, as shown in Figure 9. At higher altitudes, on the contrary, it is the **initial uncertainty in the semi-major axis** the limiting factor. **Moreover, as the number of observable objects at a given altitude increases, the initial semi-major axis uncertainty becomes more and more relevant, even at low altitudes.**

The accuracy in the semi-major axis can be increased not only by increasing the system sensors accuracy but also with the orbit determination algorithm used for initial orbit determination. Some studies [7] show that the reference figure of 100 m taken for the initial semi-major axis uncertainty resulting from an initial orbit determination can be reduced up to the radar range accuracy (of the order of 10 m) if track-to-track correlation and orbit determination techniques are performed to initialize an object in the catalogue. In order to further reduce the drag-induced uncertainty, the prediction error in the Space weather indicators and the atmospheric models itself need to be reduced.

4.4. Eccentric orbit detection capabilities

Finally, an extended study was performed, including **eccentric objects** in the population. The results of this second analysis show that, these objects can be relevant for the system operation. Eccentric objects (eccentricity higher than 0.1) can be observed also by the radar with **revisits times below 7-10 days** to cover the 90% of the objects and passes durations in the range of 70 to 300 seconds. Lower radar latitudes are preferable for the observation of this type of

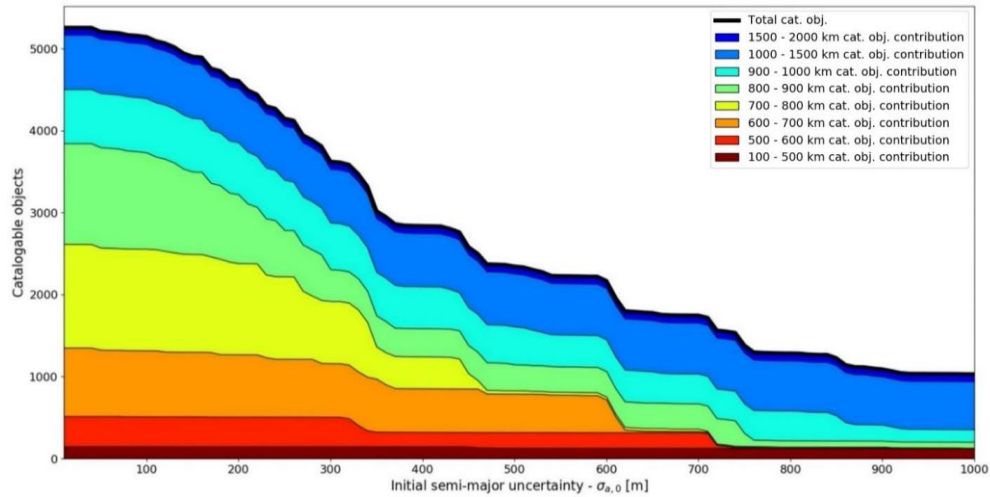


Figure 8: Evolution of catalogued objects with the initial semi-major uncertainty segmented by altitude (Radar 2)

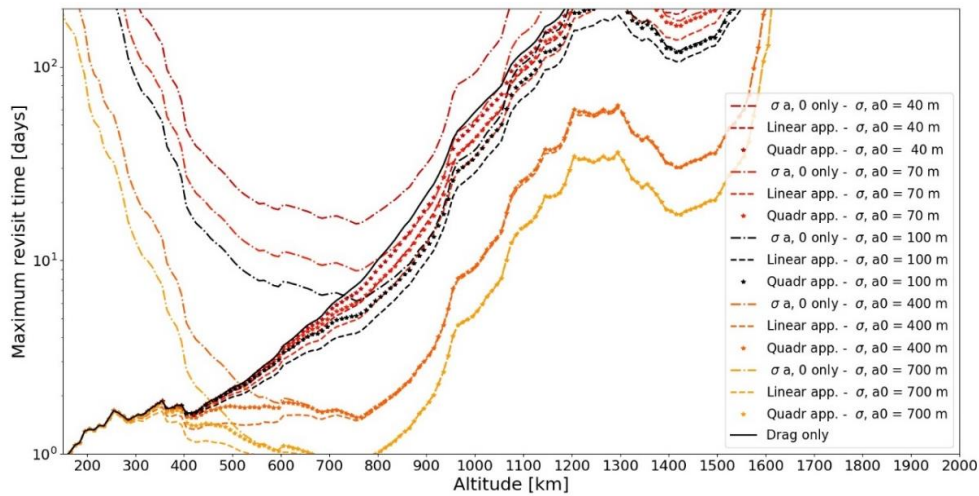


Figure 9: Initial uncertainty in the semi-major axis effect on the maximum allowable revisit time

objects. An extended study should be performed in order to determine the capabilities to catalogue these eccentric objects, as only their observability has been studied here.

5. CONCLUSIONS

The main conclusions derived from the cataloguing performance analysis are:

- The **higher the number of objects**, the more relevant the **accuracy of the sensor** is.
- For a given **sensor location and accuracy**, there is a **saturation limit** related to the number of catalogued objects, even if the number of observed objects is further increased.

- **Higher FoV pointing elevations** should be preferred in terms of **number of catalogable objects**, while **lower elevations** are more suitable in terms of **revisit time and track duration**.
- The rule-of-thumb of **1-day revisit time** for catalogable objects is **too restrictive** as it does not take into account the number of objects of the observable population and the accuracy of the sensor, among others.
- As the number of **observable objects** at a given altitude increases, the initial semi-major axis uncertainty (and thus the sensor accuracy) becomes more and more relevant, even at low altitudes

6. ACKNOWLEDGEMENTS

The authors would like to acknowledge the contributions from Alfredo Miguel Antón Sánchez and Pablo García Sánchez from GMV for their support, review and advice.

REFERENCES

- [1] H. Krag, H. Klinkrad, R. Madde, G. Sessler and P. Besso, "Analysis of Design Options of a Large Ground-Based Radar for Europe's Future Space Surveillance System," vol. 6, pp. 24-28, 2007.
- [2] G. R. Curry, Radar system performance modeling, vol. 1, Artech House, 2005.
- [3] "Report and forecast of solar and geophysical activity," National Oceanic and Atmospheric Administration, [Online]. Available: <https://www.swpc.noaa.gov/products/report-and-forecast-solar-and-geophysical-activity>.
- [4] "Space track," Joint Functional Component Command for Space, [Online]. Available: <https://www.space-track.org/>.
- [5] L. Sagnieres and I. Sharf, "Uncertainty characterization of atmospheric density models for orbit prediction of space debris," *7th European Conference on Space Debris*, 2017.
- [6] L. A. C. Pardini, "Comparison and Accuracy Assessment of Semi-empirical Atmosphere Models through the Orbital Decay of Spherical Satellites," 2001.
- [7] J. Siminski, "Techniques for assessing space object cataloguing performance during design of surveillance systems," pp. 14-17, 2016.
- [8] I. Alonso Gómez, S. Ansorena Vildarraz and e. al, "Description of the architecture of the Spanish Space Surveillance and Tracking System," *5th European Conference on Space Debris*.
- [9] K. F. Tapping, "The 10.7 cm solar radio flux (F10.7)," *Space Weather*, vol. 11, pp. 394-406, 7 2013.
- [10] "F10.7cm Radio Emissions," Space Weather Prediction Center - National Oceanic and Atmospheric Administration, [Online]. Available: <https://www.swpc.noaa.gov/phenomena/f107-cm-radio-emissions>.
- [11] S. W. P. Center, "The Planetary k-index," [Online]. Available: <https://www.swpc.noaa.gov/products/planetary-k-index>.
- [12] L. A. C. Pardini, "Comparison and Accuracy Assessment of Semi-empirical Atmosphere Models through the Orbital Decay of Spherical Satellites," 2001.
- [13] C. Pardinia, W. K. Tobiskab and L. Anselmoa, "Analysis of the Orbital Decay of Spherical Satellites Using Different Solar Flux Proxies and Atmospheric Density Models," 2001.
- [14] A. Pastor, "Orbit determination for track-to-track association," Master Thesis, 2017.